13D.6

10-YEAR CLIMATOLOGY OF TROPICAL RAINFALL CHARACTERISTICS FROM TRMM DATA

Tetsuo Nakazawa *[1] and Kavirajan Rajendran [2]

1 Meteorological Research Institute, Japan Meteorological Agency
2 Centre for Mathematical Modelling & Computer Simulation,
National Aerospace Laboratories, India

ABSTRACT

Using TRMM 3A25 data from December 1997 to the present, we examined the interannual variation of the rainfall characteristics in the tropics globally and locally. The result shows that the TRMM 3A25 data and other TRMM data detect the interannual variation of rainfall over the tropics, in concert with the SST change, which is closely related with El Niño/La Niña cycle.

We examined the impact of the altitude boost of the satellite from 350 km to 400 km in August 2001, and found that the boost affects little to the interannual variation.

1. INTRODUCTION

Tropical Rainfall Measurement Mission (TRMM) satellite was launched in November 1997 to measure precipitation over the tropical area (37 ˚N – 37 ˚S) by several sensors. The Precipitation Radar (PR), developed in Japan, is one of the key sensors to provide vertical profiles of rain over the tropical land and ocean areas.

In August 2001, the satellite was boost up from 350 km to 400 km in altitude to extend its life. As the PR is an active sensor, it is expected that the sensitivity would be degraded due to the boost. To understand the interannual variation we have to evaluate the impact of the boost (Robertson et al, 2003). In addition, the timing of the boost coincides with the period of the phase shift from the La Niña to El Niño period. Thus it is important to separate the impact of the boost from the ENSO cycle.

With the above objectives, we analyzed the TRMM PR 3A25 dataset, which includes not only the monthly mean rain rate, but also many statistical values, such as monthly histograms of rain rates (total, convective, stratiform), storm height etc. at each 5 degree longitude/latitude box.

2. 3A25 DATASET

TRMM PR 3A25 version 6 dataset (Iguchi et al., 2000) provides various statistics of conditional rain characteristics over a month from the level 2 PR products. The dataset contains, for example,

- mean, standard deviations and count values
- histograms
- correlation coefficients

and RZ coefficients, a and b for $R= AZ^b$

There are two horizontal resolution datasets in the 3A25, 0.5x0.5-degree and 5x5-degree. In this study, we have only used 5x5-degree product.

3. RESULTS

3.1 *From La Niña to El Niño*

First of all we see the temporal change of OLR (out going longwave radiation), shown in Fig. 1. During the period before the boost (BB, from December 1997 to July 2001), the La Niña phase prevailed, but after the boost(AB, from September 2001 to December 2007), the El Niño or El Niño-modoki (Ashok et al., 2007) phases prevail. The difference (AB-BB) shows the ENSO signal clearly, the sea-saw pattern between the maritime continent and the central Pacific. It can be seen from Fig. 1 (right) that the timing of the boost coincides with the transitional period from the La Niña to the El Niño phase.

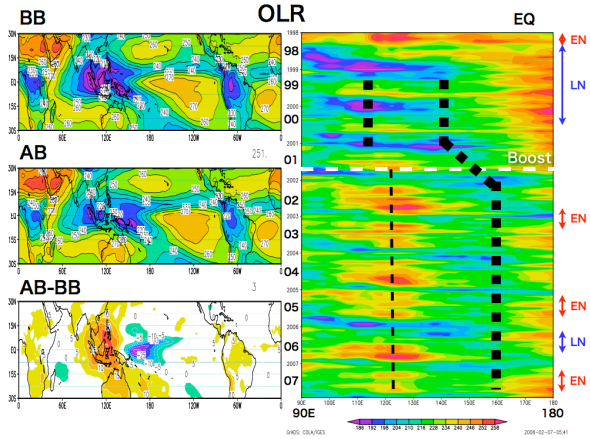

Fig. 1. (Left) OLR mean before the boost (BB) and after the boost (AB) and the difference (AB-BB). Area with cool (Warm) color denotes the area of active (suppressed) convection. (Right) Time-longitude diagram of OLR along the equator. The boost occurred in August 2001 (white dashed line). On the right EN and LN denote the phases of El Niño and La Niña.

The rain fraction is defined as the percentage of the total rain pixel numbers with total pixel numbers within each 5x5 degree box. Fig. 2 shows that the period before the boost (BB) is the La Niña phase, and the period after the boost (AB) corresponds to the El Niño phase. The histogram of occurrence of heavy rain rate (48-65 mm/h) in the estimated surface rain in 3A25

**Corresponding author address*: Tetsuo Nakazawa, Meteorological Research Institute, Japan Meteorological Agency, 1-1 Nagamine, Tsukuba, Ibaraki, 305-0052; e-mail: nakazawa@mri-jma.go.jp.

dataset, also shows the same tendency (not shown). That is, the center of the heavy rain rates along the equator has shifted eastward from the western Pacific (BB) to the eastern Pacific (AB).

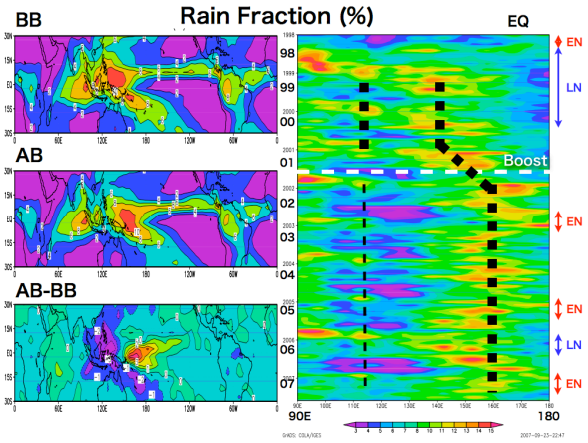

Fig. 2. Same as Fig. 1, but for the rain fraction (%).

From the above two figures, we addressed the following questions.

(1) How do the boost and the transition from La Niña to El Niño appear in the TRMM data?

(2) Can we separate these two in the TRMM data?

In this study, these questions are answered by mainly applying the EOF (Empirical Orthogonal Function) analysis to the PR 3A25 datasets from December 1997 to the latest month (December 2007).

3.2 *Temporal Change of Global Histograms of Rain*

Before applying the EOF analysis, we first examine the temporal variation of the global sum of the pixel numbers of the conditional rain rate at 2 km. Figure 3 clearly suggests that the number of pixels has sharply decreased from heavier than that based on the MTSAT 1R. It is to be noticed that the number gradually increased over the medium range (0.65 – 20.5 mm/h).

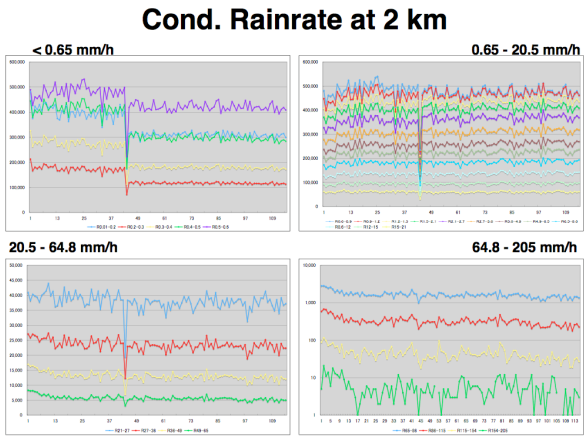

Fig. 3. Total number of pixels with conditional rain rates from weak (top-left) to heavy (bottom-right) at 2 km. The vertical axes are linear, except for the heavy histogram (54.8-205 mm/h), which is logarithmic.

3.3 *EOF Analysis for Rain Histograms with ENSO Index*

We applied EOF analysis to the following parameters in the 3A25 data.

- unconditional rain rate, convective rain rate and stratiform rain rate,
- histogram data for total rain rate, convective and stratiform rain rate of 5 classes (light to heavy rainfall) at 2 km
- SST

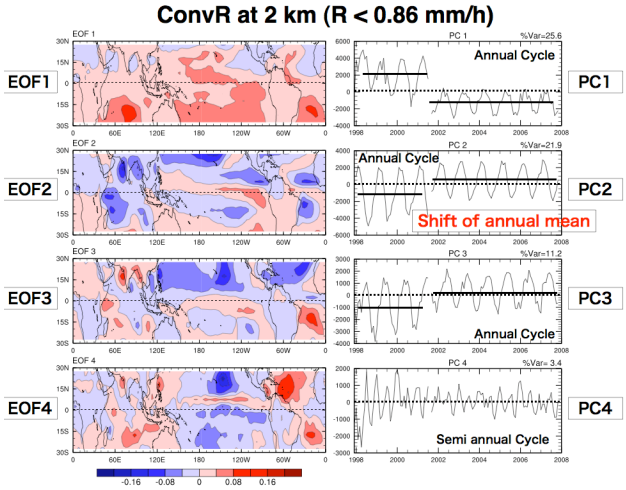

Fig. 4. EOF 1-4 (from top to bottom) spatial patterns of the occurrence numbers of convective rain rate, convrainH, with rainfall less than 0.86 mm/h (left) and the corresponding temporal patterns of PC 1-4 for the same parameters (right).

Figure 4 represents the first four EOF patterns (left) with its temporal coefficients (right) for the number of occurrence with weak convective rain rate (less than 0.86 mm/h) at 2 km. In Fig. 4, PC1 to PC3 show the clear annual cycles (wave-like patterns) but an abrupt stepwise shift of the baseline of the annual mean during the boost. Two dominant interannual conditions are evident before and after the boost in Fig. 4. The first three principal components identify both annual cycle and the abrupt change of the mean state. From the spatial patterns (Fig. 4, left) we note that the first EOF mode (EOF1) corresponds to the equatorial and the boreal winter component, and the second EOF mode (EOF2) corresponds to the boreal summer component. There are no ENSO related modes in the first four EOFs in Fig. 4.

Figure 5 shows the EOF of the occurrence number of the total rain rate less than 0.65 mm/h at 2 km. In PC1 (top right) there is a reduction in the amplitude of the annual cycle during the boost. Before the boost the amplitude of the annual cycle is larger than that after the boost. However, in PC2, the mean state changed from positive to negative, indicating the rainrate over the maritime continent is getting weaker after the boost. This interannual change can also be seen in PC3, which is the signal of the ENSO cycle. We overlay the temporal variation of the NINO 3.4 SST variation on PC3 (third from the top, right).

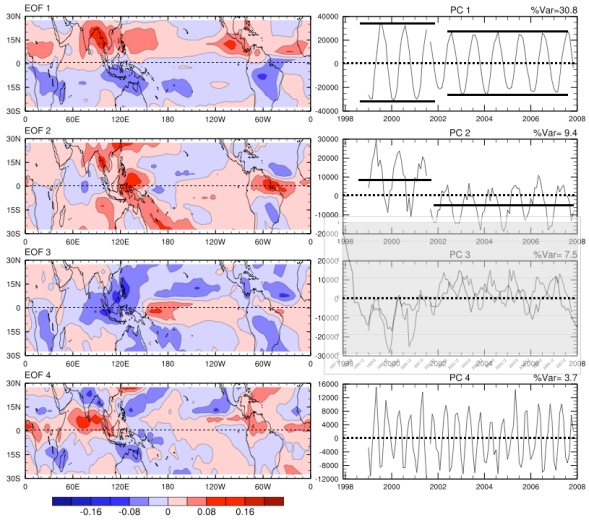

Fig. 5. Same as Fig. 4, except for the total rain rate, less than 0.65 mm/h at 2 km.

Figure 6 shows the occurrence number of the stratiform rain rate, less than 0.65 mm/h at 2 km. The PC1 in Fig. 6 is similar to that in Fig. 5, however, the reduction in the amplitude of the annual cycle in PC1 largely comes from the negative part, indicating the rainrate is getting weaker during the Northern summer. As in Fig. 5, the ENSO mode is detected in PC3.

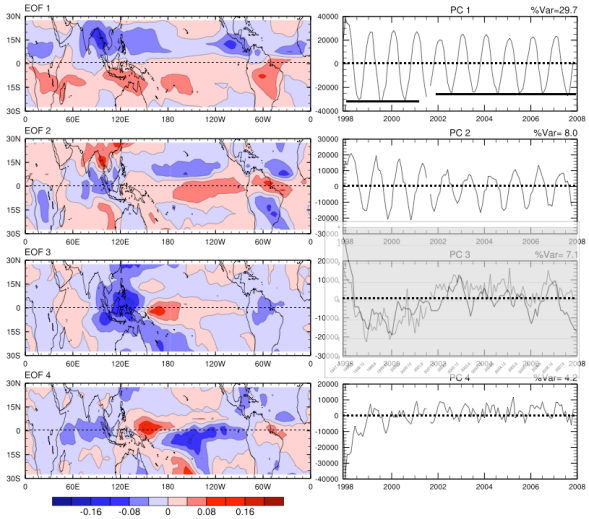

Fig. 6. Same as Fig. 4, except for the stratiform rain rate, less than 0.65 mm/h at 2 km.

3.4 *Modulation of Annual Cycle by ENSO Cycle?*

In the previous section, we examined the spatial and temporal patterns of dominant modes of the rainrate variations in the TRMM PR 3A25 10-year dataset and found that sometimes PC1 and PC2 are correlated and PC3 and PC4 as well. Thus, in this section we further analyze the variations by plotting the scatter diagrams of (PC1, PC2) and (PC3, PC4).

Figure 7 shows the scatter diagram of (PC1, PC2) and (PC3, PC4) for the occurrence numbers of convective rain rate less than 0.86 mm/h at 2 km, similar to Fig. 4. The (PC1, PC2) in Fig. 7 (left) clearly shows the transition of the mean states before the boost (BB) and after the boost (AB). We speculate that the transition reflects the boost, not the ENSO cycle. The gravity center of the annual cycle at BB (AB) shows that the PC1 >0 (<0), PC2 <0 (>0). Comparing with the spatial patterns of PC1 (positive areas are dominant) and PC2 (negative areas are dominant) in Fig. 4, we conclude that the detection of the weak rain by the PR degraded due to the boost. In contrary, the (PC3, PC4) shows the ENSO cycle. Before the boost, that is during the La Niña condition, there are large negative coefficients in PC3, than after the boost. This transition confirms the summer rainfall reduction over the Northern Hemisphere (See EOF3 in Fig. 4).

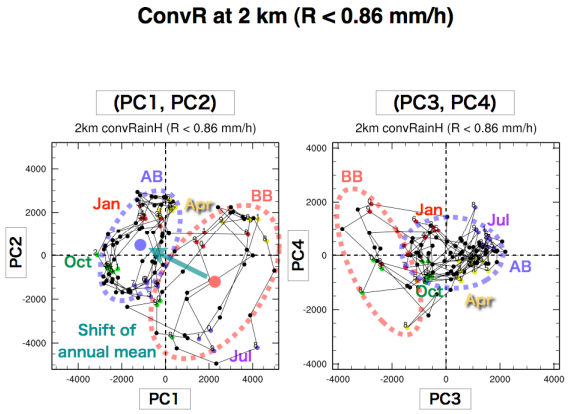

Fig. 7. Scatter diagram of (PC1, PC2) (left) and (PC3, PC4) (right) for the occurrence numbers of convective rain rate less than 0.86 mm/h at 2 km.

Figure 8 is same as Fig. 7, but for the unconditional rainrate at 2 km. It is to be kept in mind that this quantity is not the occurrence number, but the rainrate itself. In (PC1, PC2), we recognize that there is a phase shift or modulation of the annual cycle. That is, before the boost (BB), the coefficients of PC1 and PC2 were (+,-) in April and (-,+) in October. However, after the boost (AB), these were (~0, -) and (~0,+). This means that the seasonal cycle shifted by about a month and the the spring came a month later(earlier) before (after) the boost. This phenomenon would be related to the ENSO cycle.

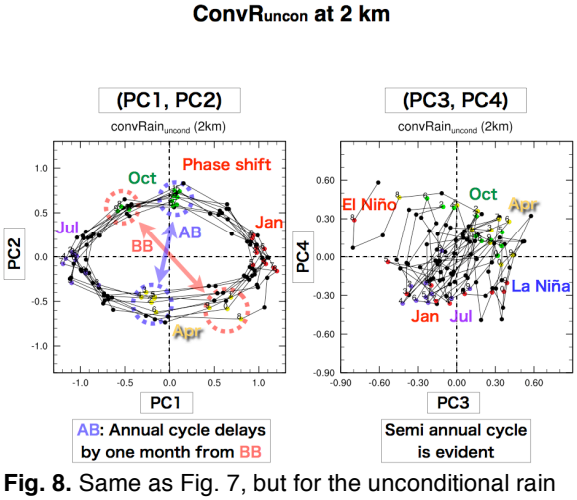

Fig. 8. Same as Fig. 7, but for the unconditional rain rate at 2 km.

We examined to see the variation in the global SST (Fig. 9). The (PC1, PC2) in Fig. 9 (left) shows the clear seasonality. However, the (PC3, PC4) shows the ENSO cycle with semi-annual variability, mainly in PC4. But in this figure, there are no such a signal of the modulation of the annual cycle, as was shown in Fig. 8.

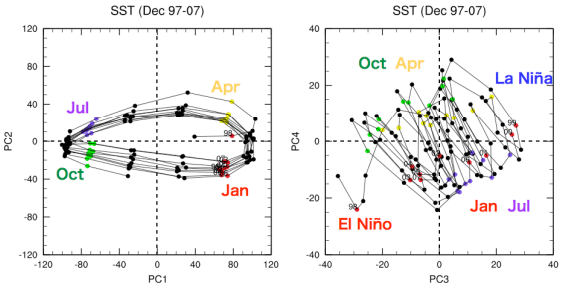

Fig. 9. Same as Fig. 7, except for the (PC1, PC2) of the global SST.

4. Summary

Using 10-year TRMM PR 3A25 dataset with many statistical representations, we described the impact of the boost and the interannual variability of the rainfall characteristics in the tropics.

By applying EOF analysis to rain rate histogram data, following basic modes have been identified.

(1) Annual cycle
(2) Interannual variations, mainly ENSO cycle
(3) Higher frequency variations (semi-annual mode)
(4) Boost Impact, especially in the light rainrates

EOF analysis is adequate to separate the boost impact from the interannual variations. We found the following signals.

(1) Shift of the annual mean state in the interannual time-scale.
(2) Amplitude change of the annual cycle
(3) Seasonal cycle shift in the annual cycle

References

Ashok, K., S. K. Behera, S. A. Rao, H. Weng, and T. Yamagata, 2007: El Niño Modoki and its possible teleconnection, *J. Geophys. Res.*, *112*, C11007, doi:10.1029/2006JC003798.

Iguchi, T., T. Kozu, R. Meneghine, J. Awaka, and K. Okamoto, 2000: Rain-profiling algorithm for the TRMM precipitation radar, *J. Appl. Meteor.*, **39**, 2038-2052

Robertson, F.R., D.E. Fitzjarrald, and C.D. Kummerow, 2003: Effects of uncertainty in TRMM precipitation radar path integrated attenuation on interannual variations of tropical oceanic rainfall, *Geophys. Res. Let.*, **30**.